Selecting the Correct Electromagnetic Inspection Technology

Thomas W. Krause*, P. Ross Underhill

Department of Physics and Space Science, Royal Military College of Canada, Kingston, ON, K7K7B4, Canada

*Corresponding author: Tel: (001) (613) 541 6000; E-mail: thomas.krause@rmc.ca

Received: 27 August 2018, Revised: 09 January 2019 and Accepted: 11 January 2019

DOI: 10.5185/amlett.2019.2262
www.vbripress.com/aml

Abstract

Eddy current (EC) technology for inspection of conducting materials is a potential solution when conditions preclude the application of other methods. Such conditions include presence of sound absorbing coatings, unavailability of a couplant, multiple conducting layers with air gaps, limited access or near surface cladding. However, the choice of a particular EC technology may not be clear due to sources of electromagnetic interference, choice of probe design, target configuration or even available equipment. In addition, the choice of EC based technologies is extensive, including conventional EC, low frequency EC, remote field EC and pulsed EC. Each of these technologies has its own challenges and limitations, which need to be considered prior to a commitment to system development. Probe choice becomes a function of the particular technique that has been selected and may include ferrite core sensing coils, GMRs or eddy current coil array. Finally, EC signal analysis methods need to be selected based on effects of potentially multiple varying parameters. This paper examines the potential of electromagnetic inspection technology, discussing its limitations, effects of common essential parameters and analysis methodologies. Examples of recent technology applications are given and the benefits and limitations of various technologies are compared and discussed.

Keywords: Eddy current testing, pulsed eddy current testing, low frequency eddy current testing, remote field eddy current testing, electromagnetic inspection, non-destructive evaluation.

Introduction

The selection of an inspection technology for a particular application requires consideration of available or existing technologies as well as careful examination of inspection conditions in light of potentially confounding factors including accessibility, economic considerations and human factors. Examples of particular interest include inspection of conducting structures that are insulated, such as piping, for chemical processing or petrochemical industries, naval structures, coated storage vessels and nuclear reactor components. Electromagnetic inspection technologies are often only considered after more conventional techniques, such as ultrasonic and X-ray, have been ruled out, due to challenges with application or increased economic costs. However, the limitations of electromagnetic technologies and potential pitfalls for their application may not be well understood and may lead to unexpected effects that limit or may even negate their effectiveness. Therefore a comprehensive understanding of the potential and limitations for application of electromagnetic inspection is required.

Eddy current (EC) testing is based on Faraday's law of electromagnetic induction and was first applied as a testing technique in 1879 when D.E. Hughes used changes in electromagnetic response to distinguish different metals based on resistivity and magnetic permeability [**1**]. EC testing has become a standard inspection method with applications that range from measuring changes in resistivity and permeability, detecting defects, and measuring thickness of conducting and nonconducting coatings [**1**-**3**]. Inspection applications arise in a broad range of industries, and include nuclear reactor components, aerospace structures, oil and gas pipelines, insulated pipe for chemical processing, metallurgical processing and naval structures. The technology has seen recent advancements, primarily driven by inspection of nuclear steam generators, with development of EC arrays for more rapid inspection capability [**4**], combined with multi-frequency mixing for flaw detection [**4**] and analysis of signals [**5**]. For applications in nuclear fuel channels, novel surface profiling [**6**], and proximity measurement through conducting plates [**7**] and tubes [**8**, **9**] have also recently been implemented. Dent depth measurement has also been developed for composite honeycomb aerospace structures [**10**]. Recent technological developments in EC instruments have allowed lower frequencies than the ~1 kHz, which was

previously the minimum frequency provided by most EC instruments. This has permitted development of an inspection capability for thick conducting aluminum aerospace structures at frequencies of 200 Hz and has been referred to as low frequency eddy current (LFEC) [**11**].

Remote field eddy current (RFEC) has also seen recent development from its original application to tubular ferromagnetic tubes [**12**] to that of flat plates by applying thick shielding around excitation coils [**13**, **14**]. For nuclear applications, shielding has been used to enhance far side detection in tubes [**15**]. In addition, RFEC has been applied to remote detection of conducting structures from within nuclear fuel channels [**16**]. Development of RFEC has recently seen enhanced signal analysis by removal of double-peak signal for tubular inspections [**17**].

Pulsed eddy current (PEC) uses a square pulse excitation to induce a transient electromagnetic field response from conducting components, in contrast to the sinusoidal excitation used in conventional or remote field EC. Square pulse excitation in PEC can be viewed as a spectrum of discrete frequencies, with the lowest frequency affording the greatest depth of penetration. The resulting sensed responses can come from deep within conductors [**18**-**20**] and at large liftoffs [**21**, **22**], for application to aerospace wing structures, and also insulated pipe inspection [**23**]. In the case of long pulses the approach-to-constant field also permits ferromagnetic materials to act as conduits for magnetic flux, allowing for magnetization to greater depths and interactions at large distances for remote conducting materials [**24**, **25**]. In conducting ferromagnetic materials this also results in transient field decay times on the order of many milliseconds, which again effectively corresponds to low frequencies and, as a consequence, greater depth of penetration. At long times decay rate is primarily exponential, which simplifies signal analysis [**22**, **23**, **24**]. PEC has been shown to be capable of detecting hidden corrosion in conducting multilayer aircraft structures [**26**, **27**]. Compensation for variation in lift-off and gap in multi-layer components has been developed [**28**, **29**]. PEC has also been developed to measure acoustic tile thickness up to 40 mm on submarine hull to within 0.5 mm [**30**] and through carbon-fibre/epoxy composite wing skin, of varying thickness (6 to 21 mm), for crack detection in Al wing spars of F/A-18 aircraft [**21**, **22**, **31**]. PEC signals have been analyzed using a multivariate statistical analysis technique, Principal Components Analysis (PCA), to isolate various elements in the induced transient eddy current signal [**21**, **22**, **24**, **31**-**33**]. Recent work has demonstrated the ability to separate out effects of nonferromagnetic conducting materials from ferromagnetic support structure corrosion as inspected from within nuclear steam generator (SG) tubing [**34**]. Application of cluster analysis to PCA scores has shown potential for identification of various loose part materials located on the top of tube sheets as detected from within nuclear SG tubes [**35**].

This paper provides an overview of the state-of-the-art in eddy current testing, identifying its potential applications, advantages over other inspection techniques, and limitations with potential pitfalls. Goals for electromagnetic testing include detection of flaws at depth in conducting structures, measurement of remaining wall thickness under general corrosion conditions, remote detection through nonconducting media, measurement of conductor proximity and identification of materials. This paper will examine the various eddy current inspection technologies (EC, LFEC, RFEC and PEC) that can be used to perform these types of measurements, along with consequent trade-offs in resolution and sensing capability for the different methods. An overview of more recent developments will be presented along with prospects for future applications.

Eddy current testing theory

The modified wave equation for electric fields, $\boldsymbol{E}$, in matter is expressed as [**36**, **37**],

$$\boldsymbol{\nabla}^2\boldsymbol{E} = \mu\sigma\frac{\partial \boldsymbol{E}}{\partial t} + \mu\epsilon\frac{\partial^2 \boldsymbol{E}}{\partial t^2}, \quad (1)$$

where, σ is the conductivity, μ is the permeability and ϵ is the permittivity. In a nonconducting volume where conductivity is zero the electromagnetic fields are described by the wave equation,

$$\boldsymbol{\nabla}^2\boldsymbol{E} = \mu\epsilon\frac{\partial^2 \boldsymbol{E}}{\partial t^2}. \quad (2)$$

In a conducting volume, where Ohm's law applies, the time dependent electric fields are proportional to current densities according to $\boldsymbol{J} = \sigma\boldsymbol{E}$. In metallic conductors, at less than microwave frequencies (GHz), where $\sigma \gg \epsilon\omega$, equation 1 may be written as the diffusion equation [**38**].

$$\boldsymbol{\nabla}^2\boldsymbol{J} = \mu\sigma\frac{\partial \boldsymbol{J}}{\partial t}. \quad (3)$$

Under time harmonic conditions the time dependent current density is expressed as

$$\boldsymbol{J}(t) = \boldsymbol{J_0}e^{i\omega t}, \quad (4)$$

where, $\boldsymbol{J_0}$ is the maximum current amplitude and ω is the radial frequency. For a plane wave incident on a conducting half-space, normal to the z-axis the solution to equation 3 becomes

$$\boldsymbol{J} = \boldsymbol{J_s}e^{-\frac{z}{\delta}}e^{i(\frac{z}{\delta}-\omega t)}, \quad (5)$$

where, $\boldsymbol{J_s}$ is the surface current density and δ is the skin depth given by

$$\delta = \sqrt{\frac{2}{\mu\sigma\omega}}. \quad (6)$$

Note that the first exponential on the right hand side of equation 5 refers to the attenuation of the current density into the material, while the second exponential, refers to the increased time or phase lag of the sinusoidal signal with depth into the conductor.

Fig. 1 shows a representation of a planar time-harmonic electric field incident on a conducting half space, and resulting exponential decay of eddy currents with depth into the conductor.

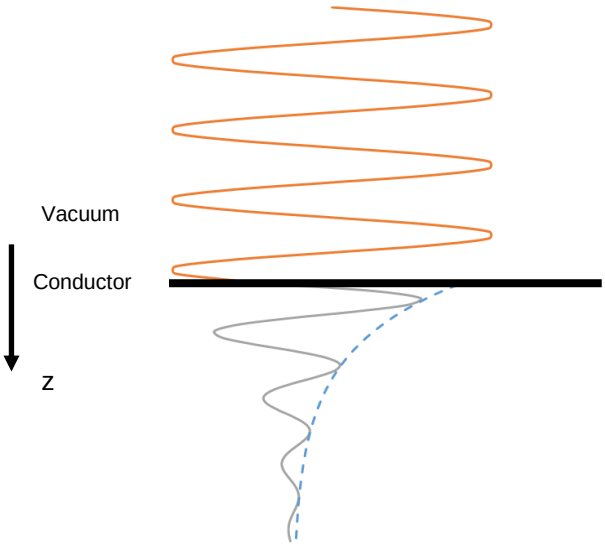

Fig. 1. Representation of planar electric field wave incident on conducting half space and its exponential decay into the conductor.

Under conditions where the field excitation is not time harmonic, but rather a single square pulse, as in pulsed eddy current, transient decay of the induced eddy currents takes place. The general solution for the diffusion of currents according to equation 3 in conducting media is of the form [**39**]

$$\boldsymbol{J}(t) = f\left(e^{-t/\tau_D}\right), \tag{7}$$

where, τ_D is a characteristic diffusion time, with the solution often being expressed as a series of relaxation times, thereby producing a reasonable dependence of induced eddy current fields on the material conductivity and permeability [**39**]. The diffusion time τ_D for these transient eddy currents in a given material can be described by [**37**, **39**]

$$\tau_D \sim \mu\,\sigma\,\ell^2, \tag{8}$$

where, ℓ is a characteristic length of the system. The complete transient response can be understood as a series of discrete relaxation times described by equation 8, with longer times resulting in greater depth of penetration by eddy current fields. Equation 8 can be reconfigured into an equivalent expression for the greatest skin depth under transient conditions given by [**40**]

$$\delta \sim \sqrt{\frac{\tau_D}{\mu\sigma}}, \tag{9}$$

where, the characteristic length, ℓ, has now been considered as the effective skin depth at the longest relaxation time.

Sensing of conducting material property changes, including the presence of flaws, resistivity changes, conductor proximity or changes in geometry, is accomplished by using an eddy current coil sensor. The voltage induced in a sensing coil in the presence of a time varying field arises according to Faraday's law as

$$V = -N\frac{d\Phi}{dt}, \tag{10}$$

where, Φ is the magnetic flux through a pickup coil with N turns.

The solution for the direct response between a coil, excited by a constant amplitude alternating current, and conducting sample for both an infinite layered conductor and layered rod with encircle coil was first provided by Dodd and Deeds [**38**]. Their work [**38**] also facilitated modeling and prediction of coil response for a finite rectangular coil with ability to predict lift-off response and the reduction in penetration depth due to finite coil size. For example, **Fig. 2** shows the effect of coil size on depth of penetration into Al 7050-T76 (σ = 23 MS/m), obtained here using COMSOL finite element method modeling software. The development of an analytical model also permitted the advance towards a rigorous formalism to display and interpret eddy current data [**1**-**3**]. The single coil or coaxial driver-pickup coil pair is most sensitive to lift-off and has been used for measuring paint thickness [**1**-**3**] or more recently, for profiling dents in aluminum skin honeycomb panels [**10**]. Advances in modeling have also provided the means to evaluate the generation of eddy currents as a single coil passes over a flat planar edge [**41**].

Sensing of conductive material property changes including presence of flaws, resistivity changes, conductor proximity or changes in geometry is most often accomplished using pairs of eddy current coil sensors. One coil generates a time varying magnetic field, the drive coil, and a second, the pick-up coil, senses it. This transmit-receive technology has been applied extensively in the nuclear industry [**42**].

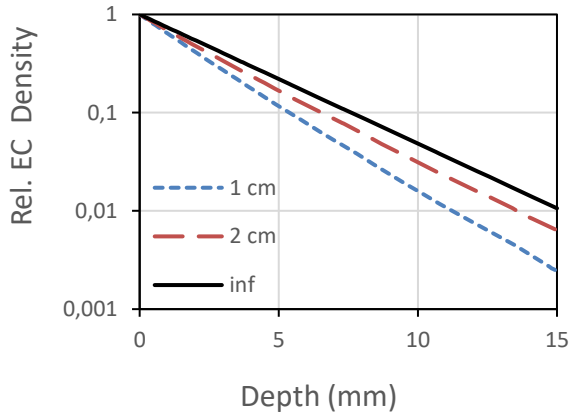

Fig. 2. Relative eddy current density as a function of depth into Al 7050 T76 for coils of 1 cm, 2 cm and infinite (inf) diameter (Coil results are from COMSOL FEM simulation).

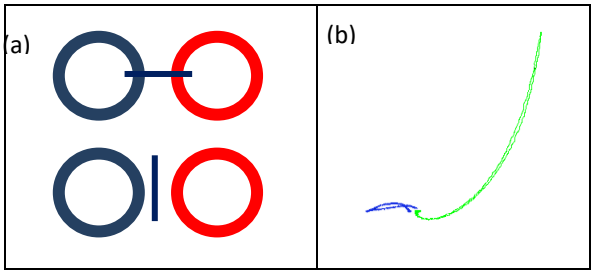

Fig. 3. (a) Effect of crack orientation on transmit-receive sensitivity. (b) Green curve in the impedance plane display on right corresponds to crack-to-probe alignment at the top left. Blue curve on the right corresponds to crack alignment on bottom left. Lift off is horizontal to the left, overlapping the blue curve.

Transmit-receive eddy current probes have benefits over single eddy current coils, including improved signal-to-noise ratio in the presence of varying lift-off and temperature, directional sensitivity and capability to optimize coil size and spacing for a particular application [**4**]. Transmit-receive probes are primarily sensitive to cracks lying in the gap between the coils and running between the two coils as shown in the top left of **Fig. 3(a)** with corresponding response in **Fig. 3(b)**. Cracks oriented in this manner cut the maximum amount of eddy currents.

Analytical models have been formulated for transmit-receive configuration [**43**]. More recently Burke and Ibrahim [**44**] developed exact solutions for mutual inductance of a transmit-receive probe above a conductive plate. Note that pick-up coil response as well as drive coil field are affected by each other through direct interactions (mutual inductance, M), interactions with themselves (self-inductance, L), and by interactions of each coil with the conducting test piece (lossy inductance, $\mathcal{L}$) and between coils via the conducting test piece (lossy inductance, $\mathcal{M}$) [**45**]. This multiply-connected process is shown in **Fig. 4**. Analytical models that incorporate all of these electromagnetic interactions have recently been developed for EC transmit-receive probe configurations, applied to layered infinite planar conductors [**7**] and from within concentric tubes [**9**].

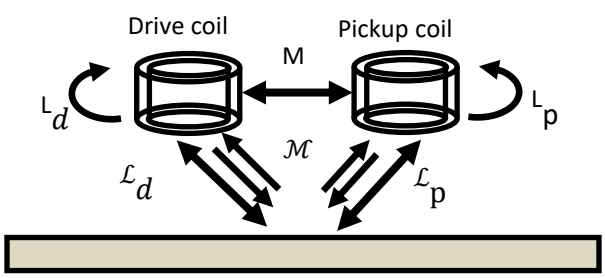

Fig. 4. Electromagnetic interactions between drive (d) and pickup (p) coils (mutual inductance, M), by interactions of coils with themselves (self-inductance, L) and self-interactions between coils and conductive test piece (lossy self-inductance, $\mathcal{L}$) and between coils via the sample (lossy mutual inductance, $\mathcal{M}$).

Probe design

Probe design plays a critical role on whether or not target inspection requirements can be met. Although fundamentally based on the same physical principle of electromagnetic induction, the various classes of eddy current testing typically use different probe configurations. While only conventional eddy current may still use a single absolute impedance coil, even this probe is often set up against a second reference coil that may be mounted against a dummy sample in order to minimize the effects of thermal drift [**1-3**]. The majority of inspection applications now use a transmit-receive configuration that consists of a driver and one or more pick-up coils. Transmit-receive probe configurations are directionally dependent (see **Fig. 2**), making it possible to target particular flaw orientations, such as circumferential and axial cracks [**4**, **42**, **46**]. The pick-up coils may be connected individually (absolute mode) or as pairs with signals subtracted (differential mode). While absolute probes are sensitive to gradual material changes, differential pick-up configurations are more sensitive to abrupt changes, such as may arise due to cracks or flaw edges [**1-3**]. The differential configuration is also less sensitive to lift-off variations and thermal drift. A drive coil that is significantly larger than the receive coil has typically been used for RFEC [**12**] and PEC [**30**, **47**] applications. The large coaxial drive coil in RFEC tube inspection applications results in a double signal, since separate responses arise as driver and pick-up pass over a defect [**12**, **17**]. This requires more complicated signal analysis and limits resolution due to the greater field spread. Extended fields can also increase the dependence on essential parameters, such as varying tube wall thickness or resistivity. Limited resolution becomes a challenge for PEC probe designs due to field spread at large liftoffs [**30**]. Both EC and PEC probe configurations benefit from ferrite cores, since this amplifies the magnetic flux within the drive coil, with a consequent increase in field strength. Design of PEC probes, however is differentiated from EC time-harmonic designs, since the circuit relaxation time defined by the ratio of resistance to inductance (R/L), plays a role in determining the frequency spectrum of the PEC probe [**40**]. Probe designs have been optimized by both finite element method [**47**] and analytical [**48**, **49**] modeling.

Signal analysis methods

Basic signal analysis in EC testing is a well-established formalism that utilizes the impedance plane display and measures amplitude and phase of signals relative to lift-off [**1-3**]. Multiple frequencies (typically up to 4) can be used to make use of linear superposition of eddy current signal response from conducting materials, permitting multi-frequency mixing of signals for removal of response from ferromagnetic tube supports and tube dents for clear identification of defect signals [**4**, **5**]. However, the number of frequencies available and their

response to each of a number of potential essential parameters (for example, superposed signals from support plates, dents, magnetite and flaws) places limitations on the effectiveness of present signal analysis methods [**4**]. For EC analysis under variable multi-parameter conditions other methods that have been investigated include PCA [**50**], and nonlinear regression feature extraction and neural networks [**51**]. Another ongoing area of research in EC signal analysis is solving inverse problems, i.e. mapping measured signals to flaws [**52**, **53**] or other material parameters. RFEC signal analysis often uses impedance plane display [**12**, **54**]. However, signal analysis is confounded by the presence of the secondary peak response, but methods that subtract this have been investigated [**17**].

Pulsed eddy current signals have conventionally been displayed in the time domain with examination of transient pulse features such as time-to-peak, time-to-zero crossing and lift-of-intersection point [**29**]. However, with regards to steel wall thickness measurements, exponential decay, as described by the generalized equation 7 has been used [**48**], which becomes a power law if multiple relaxation times are present [**55**]. Under more complex variable multi-parameter conditions more sophisticated multi-variate statistical methods have been applied, including PCA [**33**], and a modified PCA for detection of cracks at liftoff in the wing spars of F/A-18 aircraft [**31**]. These methods have been extended with the application of cluster analysis to the detection of cracks around ferrous fasteners in the wing structures of P3-Orion aircraft [**24**, **25**], and detection and identification of loose parts on tube sheets from within SG tubes [**35**]. Modified PCA has been investigated for inspection of SG tubes at support plates [**34**]. Modified PCA has also been combined with machine-learning tools such as neural networks [**56**] and support vector machine [**57**], for examination of simultaneous multi-parameter conditions in SG tube inspection. Projection to latent structures, PLS, has also been investigated as an analysis tool for wall thickness measurements [**48**].

Applications

While numerous examples of electromagnetic inspection applications are given in the literature, a few examples exhibiting state-of-the-art inspection capability and novel applications with comparison of different techniques will be presented and discussed here. Currently available EC array probes are primarily based on transmit-receive configurations. An array probe (Olympus), with 3.5 mm diameter coils, arranged in two rows, was operated here at 400 kHz. Results are shown in **Fig. 5**. The high frequency resulted in smaller depth of penetration and higher sensitivity to lift-off as measured on two honeycomb composite samples, paneled with two different thicknesses of Al containing various dent depths. In contrast to normal eddy current practice (**Fig. 3(b)**), EC phase angle was rotated so that lift-off direction was at -90 degrees in the Lissajou plot.

A less common application for EC and RFEC is measurement of the proximity of remote conducting structures. A particular example, where both technologies have been developed, is measurement of distance to Linear Injection Shutdown System (LISS) nozzles from within fuel channels of CANDU® (CANada Deuterium Uranium) nuclear reactors [**16**, **58**]. LISS nozzles are horizontal tubes that pass perpendicularly under fuel channels, consisting of a pressure tube (PT) that is contained within a larger diameter calandria tube (CT). The weight of uranium fuel bundles, radiation and ~300 °C temperatures cause the fuel channels to sag towards the LISS nozzles, with the potential for contact and consequent fretting damage. RFEC (166 mm spacing of driver and pickup) measurement demonstrates sensitivity to LISS nozzles out to 70 mm from the pressure tube, but with measurement accuracy for proximity of ±4 mm [**16**]. In contrast, a conventional transmit-receive probe with 25 mm separation is only sensitive out to 25 mm, but with better resolution in this range, giving it an estimated accuracy of ±2 mm [**58**]. In this particular case, this is of significance, since monitoring of LISS nozzle proximity only becomes important at distances less than 15 mm from the pressure tube [**16**]. A recent novel application of eddy current is the remote detection of metal level in pyrometallurgical furnaces [**62**, **63**]. In this instance, electrically conducting molten metal level was detected to within 5 mm, through the ceramic furnace wall at a 300 mm distance from the molten metal. The high resolution is a result of signal analysis using projection of latent structures, integrated over the probe's passage over the single extended feature of the molten metal edge [**63**].

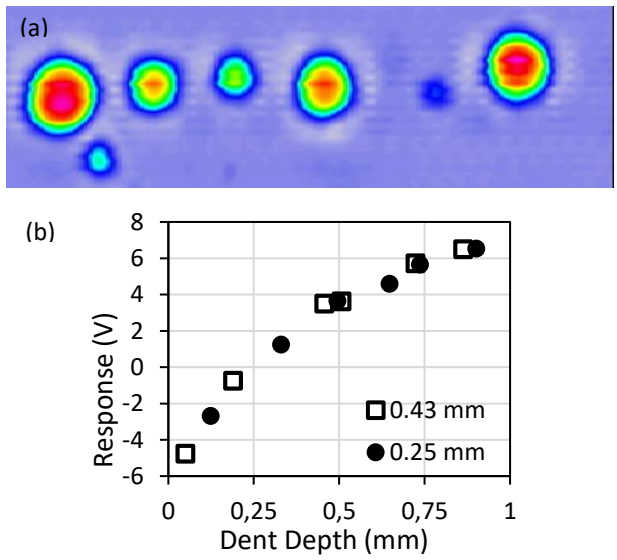

Fig. 5. (a) C-Scan display generated by EC array operated at 400 kHz obtained from range of dent sizes and depths on an Al honeycomb panel. (b) Response as a function of dent depth for two sheet thicknesses 0.25 and 0.43 mm.

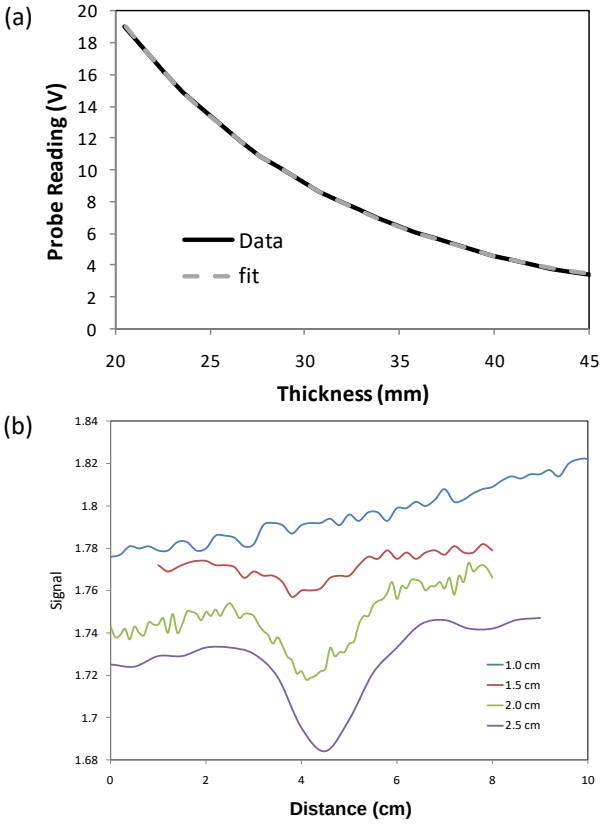

Fig. 6. (a) Comparison of calibration data and exponential fit. (b) Line scans of holes with different diameters as shown. Each hole was 3 mm deep. Scans have been shifted vertically for clarity.

PEC has also been used to achieve high resolution stand-off measurement, with 0.5 mm accuracy to two standard deviations, at lift-offs of 35 mm [**30**, **59**]. The particular application was acoustic tile thickness measurement on submarines. Laboratory tests with the differentially tuned probe demonstrated that when the signal level was adjusted to 0.1 V/mm at a lift-off of 35 mm, the noise level corresponded to only 0.03 mm [**30**]. The signal increased approximately exponentially with inverse lift-off distance, as shown in **Fig. 6(a)**, so the signal-to-noise ratio was substantially better at shorter lift-offs [30]. This is considerably better range than that reported using a multi-frequency EC lift-off measurement system by Sun *et al.* [**60**], which only extends up to 6 mm lift-off and that patented by Davies [**61**] for coating thickness measurement applications, which is only reported to 5 mm. The PEC probe's spatial resolution was sufficient to detect a 1.5 cm diameter, 3 mm deep hole in a steel plate as shown in **Fig. 6(b)**.

Discussion

This overall examination of the capabilities of eddy current testing techniques, including conventional EC, LFEC, RFEC and PEC, in light of general electromagnetic principles, can be used as a guide to identify the most suitable inspection technology given the physical parameters of a particular inspection configuration. These capabilities may be identified with regards to the skin depth (equation 6), various analytical [**38**, **45**] and FEM [**32**] modeling analyses, and a general understanding of the interaction of coil generated fields, sensors and target conductors. For example, conventional eddy current has strong capabilities for surface breaking flaw detection in nonferromagnetic conductors, but is challenged in ferromagnetic conductors by both skin depth and potential variations in surface initial permeability, which can produce spurious signals. EC analysis technologies have been challenged by simultaneous variation of many parameters [**56**], which basic impedance plane analysis techniques cannot easily accommodate [**4**]. EC also has high-resolution thickness measurement capability for thin coatings [**2**, **3**] and is capable of high resolution surface profiling [**6**, **7**]. For deep subsurface flaws in good conductors, lower frequencies for detection are required and these have been provided by more modern EC instruments, termed LFEC. However, the application of LFEC also incurs considerable field spread with a consequent loss of resolution, potentially weak signals from deep defects and sensitivity to nearby geometry changes, such as edges [**11**]. The through-wall inspection capability for ferromagnetic materials has been met by RFEC [**12**] and by PEC [**48**], even at large lift-offs [**23**, **34**, **55**]. The trade-offs in these cases have been a loss of resolution due to field spread and signal analysis challenges when simultaneous variation of multiple essential parameters is present [**56**]. Disadvantages also include large signal amplification requirements and removal of noise. Applications, target materials and potential limitations for each of these techniques are summarized in **Table 1**.

Table 1. Summary of electromagnetic techniques indicating applications, materials and limitations.

Technique	Applications	Limitations
Eddy Current	-Freq. 2 kHz to 10 MHz -Flaw detection surface and near surface -Thickness measurement -Resistivity measurement -Surface profiling -Metal detection	-Skin depth limited -Ferromagnetic[1] -Depends on eddy current direction -Field spread ~4δ -Edge effects
Low Frequency Eddy Current	-Frequency < 2 kHz -Flaw detection at depth in good conductors (σ > 10 MS/m) -Larger lift-offs	-Edge effects -Weak response -Field spread reduces resolution
Remote Field Eddy Current	-Freq. 10 Hz to 1 kHz -Flaw detection in ferromagnetic and thick conducting tubes -Remote conducting structure detection	-Double signal -Reduced resolution -Signal amplification required
Pulsed Eddy Current	-Corrosion detection in thick ferromagnetic (< 25 mm) components -Thickness measurement at large lift-off -Remote conducting structure detection	-Signal analysis -Reduced resolution -Signal amplification required

[1]Skin depth and sensitive to surface permeability variations.

In summary, selection of the most effective electromagnetic inspection technology depends on the

particular application and material. For example, referring to **Table 1**, considerations are: Is the application a surface inspection (EC), does it require subsurface detection of discontinuities in a good conductor (LFEC), involve remote detection or proximity measurement of a conducting structure, and what is the resolution required? In addition, selection of the most appropriate technology may be guided by consideration of:

1. Whether ferromagnetic material is present,
2. target material's conductivity (σ > or < 10 MS/m),
3. proximity of the probe to the test piece, and
4. whether geometrical changes in the component are close to the sensing probe. Suggested selection of the most appropriate electromagnetic inspection technology, in light of general material properties, is shown schematically in **Fig. 7**.

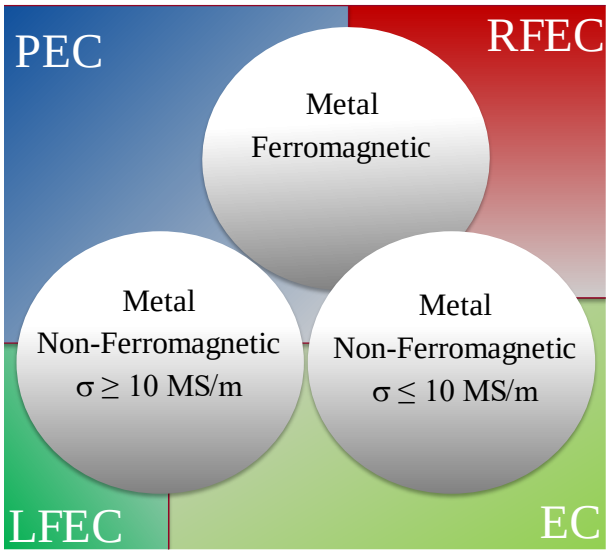

Fig. 7. Schematic representation of material classification and suggested selection of electromagnetic inspection technology.

Conclusion and future perspectives

This paper has presented an overview of the state-of-the art of various electromagnetic inspection technologies. Physical principles behind their application have been presented in order to point out inspection limitations arising due to skin depth and field spread, along with effects of various parameters, such as probe lift-off, material conductivity and permeability, and material proximity to the sensor. Probe design [**47**-**49**] and analysis methodologies [**32**, **41**, **43**-**45**], have also been presented.

Electromagnetic inspection technology has seen recent developments in high resolution surface profiling [**8**, **10**], inspection of thick multi-layer aircraft structures with ferromagnetic components present [**21**, **22**, **24**-**28**] and inspection of ferromagnetic pipe through insulation [**23**]. Remote detection [**35**] and proximity measurements are also rapidly developing capabilities [**30**, **31**, **58**, **59**, **62**, **63**]. Application of advanced signal analysis techniques, which enhance accuracy and capability to extract multi-parameter information are also seeing development [**35**, **50**-**52**, **56**, **57**, **63**].

Future perspective for electromagnetic based inspection capability will include enhanced field generation and sensor design for optimized resolution and sensitivity for material condition assessment. Development of advanced analysis tools using machine learning methods and advanced analytical and numerical models, for application of inverse analysis techniques will facilitate extraction of information under multi-parameter variation conditions that presently confound eddy current based inspection. These advancements will help make electromagnetic inspection technology a more effective and preferred option for inspection applications.

Acknowledgements

The preparation of this document has been supported by the Natural Sciences and Engineering Research Council of Canada, Defence Research Development Canada and by the Aerospace Research Advisory Committee through the Directorate of Technical Airworthiness and Engineering Support in the Department of National Defence, Canada.

References

1. Cecco, V. S.; Van Drunen, G.; Sharp, F. L.; Eddy current testing manual on eddy current method, Chalk River, Ontario: Atomic Energy of Canada Limited, **1981**.
2. Cecco, V. S.; Sharp, F. L.; Van Drunen, G.; Eddy Current Inspection. Metals Handbook Ninth Edition: Volume 17 Nondestructive Evaluation and Quality Control. Metals Park, OH: ASM International: USA, **1989**, 164.
3. Simpson, R.; Eddy-Current Inspection, Revised, ASM Handbook, Volume 17, Nondestructive Evaluation of Materials; Ahmad, A.; Bond, L. J. (Eds.); Materials Park, OH, ASM International: USA, **2018**, 477.
4. Obrutsky, L.; Lepine, B.; Lu, J.; Cassidy, R.; Carter, J; Eddy current technology for heat exchanger and steam generator tube inspection," Proc. 16th WCNDT. Montreal (Canada): **2004**. Proc. 16th WCNDT.
5. Horn, D.; Roiha, R.; Multifrequency analysis of eddy current data. Montreal (Canada): **2004**. Proc. 16th World Conf. NDT.
6. Shokralla, S.; Krause, T. W.; Morelli, *J.; NDT & E Int.*, **2014**, *62*, 153.
7. Luloff, M.S.; Desjardins, D.; Morelli J.; Krause, T. W.; *NDT & E Int.*, **2018**, *96*, 1.
8. Shokralla, S.; Krause, T. W.; Methods for Evaluation of Accuracy with Multiple Essential Parameters for Eddy Current Measurement of Pressure Tube to Calandria Tube Gap in CANDU® Reactors; *CINDE Journal*, **2014**, *35*, 5.
9. Klein, G.; Morelli, J.; Krause, T. W.; *NDT & E Int.*, **2018**, *96*, 18.
10. Reyno, T.; Underhill, P. R.; Krause, T.W.; Marsden, C.; Wowk, D.; *Sensors*, **2017**, *17*, 2114.
11. Alatawneh, N.; Underhill, P. R.; Krause, T. W.; *IEEE Sensors J.*, **2018**, *18*, 1568.
12. Mackintosh, D. D.; Russell, D. E.; Atherton, D. L.; Schmidt, T.R.; Remote Field Eddy Current for Examination of Ferromagnetic Tubes; *Materials Evaluation*, **1996**, *54*, 652.
13. Sun, Y. S.; Si, J.; Cooley, D.; Han, H. C.; Udpa, S.; Lord, W.; Qu, M.; Chen, M.; Zhao, Y.; *IEEE Trans. Magn.*, **1996**, *32*, 1589.
14. Sun, Y. S.; Udpa, L.; Udpa, S.; Lord, W.; Nath, S.; Lua, S. K.; Ng, S. K.; A novel remote field eddy current technique for inspection of thick walled Aluminum plates, *Materials Evaluation*, **1998**, *56*, 94.
15. Krause, T.W.; Schankula, J.; Sullivan, S.P., Eddy Current Detection of Spacers in the Fuel Channels of CANDU Nuclear Reactors. Toronto: **2002,** Twenty-Third CNS Annual Conference.

16. Craig, S. T.; Krause, T. W.; Luloff, B. V.; Schankula, J. J.; Eddy Current Measurement of Remote Tube Positions in CANDU Reactors. Montreal, Canada: **2004**. 16th WCNDT.
17. Luo, Q.; Shi, Y.; Wang, Z.; Wang, Z.; Zhang, W.; Ma, D.; *Journal of NDE,* **2017,** *36*, 1.
18. Sophian, A.; Tian, G. Y.; Menghao, F.; *Chin. Mech. Eng.* **2017**, *30*, 500.
19. Cadeau, T. J.; Krause, T. W.; *Rev. Prog. Quant. NDE* **2009**, *28*, 327.
20. Smith, R. A.; Hugo G. R.; Deep Corrosion and Crack Detection in Aging Aircraft: **2001**. Joint NASA/FAWA/Dod Aging Aircarft Conference, St Louis.
21. Horan, P.; Underhill, R.; Krause, T. W.; *International Journal of Applied Electromagnetics and Mechanics*, **2014**, *45*, 287.
22. Horan, P.; Underhill P. R.; Krause, T. W.; *IEEE Sensors Journal*, **2014**, *14*, 171.
23. Park, D. G. ; Angani, C. S.; Mb, K.; Kim, C. G.; Lee, D. H.; *J. Magn.*, **2012**, *17*, 298.
24. Stott, C.; Babbar, V. K.; Underhill P.; Krause, T. W.; IEEE *Sensors Journal*, **2014**, *15*, 956.
25. Butt, D. M.; Underhill, P. R.; Krause, T. W.; Examination of Pulsed Eddy Current for Inspection of Second Layer Aircraft Wing Lap-Joint Structures Using Outlier Detection Methods. *CINDE Journal*, **2016**, *37*, 6.
26. Smith, R. A.; Hugo, G. R.; Transient Eddy Current NDE for ageing aircraft-capabilities and limitations, **2000**, Proc. 4th Joint DoD/FAA/NASA Aging Aircraft Conference.
27. Plotnikov, Y. A.; Nath, S. C.; Rose, C. W.; Rev. Prog. Quant. *NDE,* **2002**, *21*, 1976.
28. Angani, C. S.; Park, D. G.; Kim, C. G.; Kollu, P.; Cheong, Y. M.; *Journal of Magnetics*, **2010**, *15*, 204.
29. Giguere, S.; Lepine, B. A.; Dubois, J. M. S.; *Rev. Prog. Quant. NDE,* **2001**, *13*, 119.
30. Krause, T. W.; McGregor, R.; Tetervak, T.; Underhill, R.; US Patent US9091664B2 A1, **2015**.
31. Horan, P.; Underhill, P. R.; Krause, T. W.; *NDT & E Int.*, **2013**, *55*, 21.
32. Babbar, V. K.; Underhill, P. R.; Stott, C.; Krause, T. W.; *NDT & E Int.*, **2014**, *65*, 64.
33. Sophian, A.; Tian, G. Y.; Taylor, D.; Rudlin, J.; *NDT & E Int.*, **2013**, *36*, 37
34. Buck, J. A.; Underhill, P. R.; Mokros, S. G.; Morelli, J.; Babbar, V.K.; Lepine, B.; Renaud J.; Krause, T.W.; *IEEE Sensors Journal*, **2015,** *15*, 4305.
35. Johnston, D. P.; Buck, J. A.; Underhill, P. R.; Morelli, J.; Krause, T. W.; *IEEE Sensors Journal*, **2018**, *18*, 2506.
36. Griffiths, D, J.; Introduction to Electrodynamics. Glenview: Pearson: USA, **2013.**
37. Jackson, J. D.; Classical Electrodynamics. Hoboken: John Wiley & Sons: USA, **1999**.
38. Dodd, C. V.; Deeds, W. E.; *J. of Appl. Phys.*, **1968**, *39*, 2829.
39. Ohanian, H. C.; *American Journal of Physics*, **1983**, *51*, 1020.
40. Krause, T. W.; Mandache, C.; Lefebvre, J. H. V.; Rev. Prog. Quant. *NDE,* **2008**, *27*, 368.
41. Theodoulidis, T. P.; Bowler, J. R.; *IEEE Trans. Magn.*, **2010**, *46*, 1034.
42. Obrutsky, L. S. ; Cecco, V. S.; Sullivan, S. P.; *Materials Evaluation*, **1996**, *54*, 93.
43. Sullivan, S. P.; Cecco, V. S.; Obrutsky, L. S.; Humphrey, D.; Smith, S. P.; Emde, K. A.; *Rev. Prog. Quant. NDE.*, **1998**, *17*, 283.
44. Burke, S. K.; Ibrahim, M. E.; *J. Phys. D: Applied Physics*, **2004**, *37*, 1857.
45. Desjardins, D. P. R.; Krause, T. W.; Clapham, L.; *NDT & E Int.*, **2015**, *17*, 8.
46. Obrutsky, L. S.; Sullivan, S. P.; Cecco, V. S.; Transmit-Recieve Eddy Current Probes. Mendoza (Argentina), CORENDE: Regional congress on nondestructive and structural evaluation, **1997**.
47. Krause, T. W.; Babbar, V. K.; Underhill, P. R.; *Rev. Prog. Quant. NDE,* **2014**, *33*, 1352.
48. Faurschou, K. F.; Morelli, J.; *Rev. Prog. Quant. NDE,* **2019**, *38*.
49. Klein, G.; Morelli, J.; Krause, T. W.; *Rev. Prog. Quant. NDE,* **2018**, *39*, 110006.
50. Shokralla, S.; Morelli, J.; Krause, T. W.; *IEEE Sensors Journal*, **2016**, *16*, 3147.
51. Rosado, L. S.; Janeiro, F. M.; Piedade, M.; *IEEE Trans. Instrum. Meas.*, **2013**, *62*, 1207.
52. Bernieri, A.; Ferrigno, L.; Laracca, M.; Molinara, M.; *IEEE Trans. Instrum. Meas.*, **2008**, *57*, 1958.
53. Popa, R. C.; Miya, K.; *Journal of. NDE*, **1998**, *17*, 209.
54. Fisher, J J.; Remote-Field Eddy Current Inspection. Metals Handbook Ninth Edition: Volume 17 Nondestructive Evaluation and Quality Control. Metals Park, OH: ASM International: USA, **1989**, 195.
55. Mokros, S. G.; Underhill, P. R.; Morelli, J.; Krause, T. W.; *IEEE Sensors Journal*, **2017**, *17*, 444.
56. Buck, J. A.; Underhill, P. R.; Morelli, J.; Krause, T.W.; *IEEE Trans. Instr. & Meas.*, **2016**, *65*, 672.
57. Buck, J. A.; Underhill, P. R.; Morelli, J.; Krause, T.W.; *Rev. Prog. Quant. NDE,* **2017**, *36*, 110005.
58. Bennett, P.; Underhill, P. R.; Morelli, J.; Krause, T. W.; *Rev. Prog. Quant. NDE*, **2018**, *38*, 230009.
59. Tetervak, A.; Underhill, R.; Krause, T. W.; McGregor, R.; Developments in Pulsed Eddy Current Technology for Submarine Hull Geometry Inspection without Acoustic Tile Removal. Halifax, NS, CF/DRDC International Defence Applications of Materials Meeting, **2011**.
60. Sun, H.; Plotnikov, Y. A.; Wang, C. ; Nath, S. C.; Sheila-Vadde, A. C.; US Patent 8436608 B2, **2013**.
61. Davies, C. US Patent 2002/0008511 A1, **2002**.
62. Saleem, A.; Underhill, P. R.; Chataway, D.; Gerritsen, T.; Sadri, A.; Krause, T.W.; Development of Eddy Current Probe using FEM for Matte Level Detection in Pyrometallurgical Furnaces, COMSOL Conference 2018 Boston, Newton, MA (US) Oct. 3-5, **2018**.
63. Saleem, A.; Underhill, P. R.; Chataway, D.; Gerritsen, T.; Sadri, A.; Krause, T.W.; Electromagnetic Measurement of Molten Metal Level in Pyrometallurgical Furnaces, IEEE Transactions on Instrumentation & Measurement, **2019**.

